

vation of the production of large-scale vortices in computer simulations¹⁰ of drift-wave turbulence contradicts such a notion. It can be explained in terms of the present theory that predicts isotropic cascading into smaller wave numbers. The condensation of energy at $k \rightarrow 0$ indicates a formation of large-scale vortices. This supports the convection process rather than diffusion process as the basic transport mechanism of a magnetized plasma.

Finally, we briefly discuss the effect of a magnetic shear. In the presence of a magnetic shear, Eq. (6) is valid only in a limited region near the mode rational surface. Within a Debye length from the mode rational surface $\vec{k} \cdot \vec{B}_0 \simeq 0$; hence the electrons do not obey the Boltzmann distribution as assumed here. Away from this region, the equation is valid until k_{\parallel} increases to the point where $k_{\parallel} v_{thi} / \omega_{ci} \simeq \gamma_N$ (v_{thi} is the ion thermal speed, k_{\parallel} is the parallel wave number, and $\gamma_N \simeq k^4 |\varphi|$ is the decay rate). Here the parallel ion inertia becomes important and the two-dimensionality assumption breaks down. This occurs typically at a distance of $5\rho_s$ from the mode rational surface. Hence in the presence of a magnetic shear the inverse cascade occurs until $k_{\perp} \sim (5\rho_s)^{-1}$, at which point the energy may be dissipated to the parallel motion of the ions.

We thank C. G. MacLennan for the numerical evaluation of the energy the enstrophy cascades, and Professor Y. Kurihara for valuable discussions.

After the submission of the manuscript, one of the authors (A.H.) learned that the evidence of inverse cascade of energy was also found by the numerical solution of Eq. (6) without the density gradient term.¹¹

¹R. Fjortoft, *Tellus* **5**, 225 (1953); Y. Ogura, *Phys. Fluids* **5**, 395 (1962); R. H. Kraichnan, *Phys. Fluids* **10**, 1417 (1967).

²A. Hasegawa and K. Mima, *Phys. Fluids* **21**, 87 (1978).

³Recently, Cheng *et al.* have derived an equation similar to Eq. (6) but with a finite-Larmor-radius correction [in Proceedings of the Annual Controlled Fusion Conference, Gatlinburg, Tennessee, 1978 (to be published)].

⁴If the density gradient is exponential, $\nabla \ln n_0$ is constant; hence the k matching is satisfied exactly. Otherwise there exists a mismatch on the order of $|\nabla \ln n_0 / k|$. However this does not produce any basic difficulty (except in the small- k region) since we consider a large- ω mismatch as will be seen later.

⁵R. Z. Sagdeev and A. A. Galeev, *Nonlinear Plasma Theory* (Benjamin, New York, 1969), p. 5.

⁶R. C. Davidson, *Methods in Nonlinear Plasma Theory* (Academic, New York, 1972), p. 243.

⁷A. Hasegawa, C. G. MacLennan, and Y. Kodama, to be published.

⁸Sagdeev and Galeev, Ref. 5, p. 103.

⁹W. Horton, *Phys. Rev. Lett.* **37**, 1269 (1976).

¹⁰C. Z. Cheng and H. Okuda, *Phys. Rev. Lett.* **38**, 708, 1037(E) (1977); C. Z. Cheng and H. O. Okuda, *Nucl. Fusion* **18**, 587 (1978).

¹¹D. Montgomery, private communications.

Continuous Creation and Annihilation of Coreless Vortices in ${}^3\text{He-A}$ in the Presence of a Heat Flow

Tin-Lun Ho

Department of Physics, University of Illinois at Urbana-Champaign, Urbana, Illinois 61801

(Received 3 August 1978)

The apparent incompatibility between a "spinning" texture in the bulk and the boundary condition at the surface is shown to be unreal. Topological arguments are used to show that this "incompatibility" can always be eliminated in both open and closed containers by appropriate textural arrangements. The "spinning" process in the bulk corresponds to a continuous nucleation of vortex rings. In an open geometry, these rings will flow downstream along the heat current. In a closed container, they will be devoured entirely by *stationary* singular loops at the surface.

Since the observation of the persistent oscillation in the intensity of ultrasound transmission in ${}^3\text{He-A}$ ¹ which indicates that there are periodic motions of the texture \hat{l} , three mechanisms have been proposed to explain this phenomenon. All

of them involve motions of textures driven by a heat flow—which can be considered as related to a chemical-potential gradient. These mechanisms are as follows: (i) formation of vortex textures and their continuous motions across the chemical-

potential gradient²; (ii) periodic motions of boojums³—surface point singularities in the texture—on the surface of the container; and (iii) existence of “solitons” in the bulk texture⁴ (obtained by solving the orbital hydrodynamic equation in one dimension numerically) which precess around the direction of the heat current.

While there are reasons to believe (as I shall explain shortly) that the observed oscillation is caused by “precessions” of the bulk texture similar but not necessarily identical to that of (iii), there is, however, a usual objection to this mechanism. It is known that the vector \hat{l} is pinned at the walls along the direction of the surface normal.⁵ If the textures keep spinning in the bulk but remain fixed at the boundaries, then it seems that there must be a continuous production of distortions in the texture, which will be accumulated near the surface. Why do these distortions never affect or stop the motion of \hat{l} in the bulk? In this Letter, I wish to point out that although the general “orbital phase slippage” argument [Eq. (1) below] implies that there must be “precessions” of the bulk texture, there are always configurations of \hat{l} (referred to as nonaccumulating textures), in both open and closed geometries, so that their “precessions” in the bulk never create additional distortions. As a result, the periodic motion can occur over and over again.

That (i)–(iii) are caused by a chemical-potential gradient $\nabla\mu$ (or a heat flow) can be understood from the acceleration equation of the superfluid velocity \hat{v}_s .⁶ [That (iii) can be so interpreted was pointed out by Volovik⁷ using an elegant topological argument. See also discussion (ii) in Ref. 6.] Thus

$$\begin{aligned} & [\langle \partial_t \hat{v}_s \rangle]_{av} + [\langle \partial_z \mu \rangle]_{av} \\ &= \int_0^T \frac{dt}{T} \int_0^L \frac{dz}{L} \frac{\hbar}{2m} \hat{l} \cdot \partial_t \hat{l} \times \partial_z \hat{l}, \end{aligned} \quad (1)$$

where the $\langle \rangle$ and $[]_{av}$ represent spatial and time averages, respectively. In the steady state, the average of $\partial_t \hat{v}_s$ is zero. The chemical-potential difference will cause motions of a nonuniform texture. This process can be alternatively described as follows. Let L be a straight line joining two points A and B in the fluid, and S_i^2 be the surface of a unit sphere representing all possible directions of the texture. The texture along L will map into a line $\hat{l}(L)$ in S_i^2 .⁸ Equation (1) implies that, in the steady state, the line $\hat{l}(L)$ will move on S_i^2 , sweeping out areas at a rate

determined by the difference $\mu_A - \mu_B$.⁷ Cases (i)–(iii) are just different aspects of this motion.⁹

Processes (i) and (ii) are essentially the same, since in general a vortex texture (such as a fountain texture²) will end up as a boojum on the surface. Although the periodic motions of boojums on the container’s surface (such as the curved surface of a cylinder with a heat flow along its axis) do not produce additional distortions in the bulk,³ surface roughness and especially sharp edges and corners (such as obtained by turning the circular cross section of a cylinder into a rectangular one) will act as trapping sites, hindering strongly the motions of boojums from driving the bulk texture to satisfy Eq. (1). To meet the phase-slippage requirement [Eq. (1)], it is preferable to have a “precessing” bulk texture sweeping out areas continuously in S_i^2 , but decoupled from the surface texture. Such a process, however, causes the aforementioned conceptual difficulty, which we now eliminate.

Let us first understand the origin of accumulation of distortions when the texture is phase slipping. Figure 1(a) represents a cross section Σ of a cylinder Ω with a rectangular boundary $abcdefa$. The direction of the heat flow is along the symmetry axis \hat{z} of the cylinder. We impose the constraint $\hat{l}(\vec{r}) = \hat{z}$ whenever \vec{r} is on the boundary. (Realistic boundary condition will soon be considered.) Let the images of the line segments \overline{dh} and \overline{ha} in S_i^2 be half circles γ_1 and γ_2 joining \hat{z} and $-\hat{z}$. Suppose at time $t=0$, they lie on the y - z plane as shown in Fig. 1(b).¹⁰ To satisfy the phase-slippage condition, γ_1 and γ_2 will precess about \hat{z} in the negative and positive sense as indicated in Fig. 1(b).⁷ After γ_1 (γ_2) returns to its original position, an additional $+$ ($-$) 8π area in S_i^2 has been accumulated in the rectangle $abcd$ ($fadef$), i.e., a pair of $+$ ($-$) 4π vortex is nucleated in $abcd$ ($fadef$).⁸ Or more precisely, a vortex ring is nucleated inside the cylinder Ω .⁸ Further precessions simply generate more vortex rings.

An obvious way to eliminate this accumulation of vortices is to relax the boundary condition of \overline{fa} and \overline{ab} in Fig. 1(a), so that the vortex pair can flow downstream, entering into the helium outside Σ . This immediately implies that in an open container (\overline{fa} and \overline{ab} are now opened), the texture can be nonaccumulating because all the vorticity generated can leave the container. These nucleation and elimination processes can occur simultaneously. For example, suppose the line \overline{ab} (\overline{fa}) in Fig. 1(a) maps into $-\gamma_2 - \gamma_1$ ($\gamma_1 + \gamma_2$) in

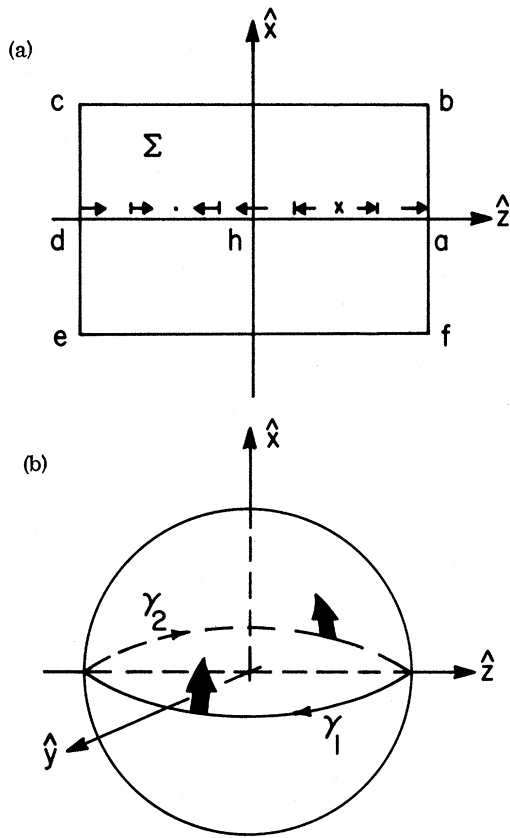


FIG. 1. (a) The cross section Σ of a cylinder Ω with symmetry axis \hat{z} . The texture along \overline{dha} at time $t=0$ is shown. The symbols \cdot and \times represent $\hat{l}=\hat{y}$ and $\hat{l}=-\hat{y}$. A vertical bar in front of or after an arrow (\hat{l} vector) indicates that the arrow is going into or coming out from the z - x plane. (b) Image loops γ_1 and γ_2 of the line segments \overline{dh} and \overline{ha} . The directions of their motions are represented by the thick arrows.

S_i^2 , where $-\gamma_1$ is just γ_1 with its orientation reversed. As γ_1 and γ_2 sweep across S_i^2 as described in Fig. 1(b), whatever positive (negative) vorticity created in rectangle $abcd$ ($fadef$) by the motions of γ_1 and γ_2 leaves $abcd$ ($fadef$) through \overline{ab} (\overline{fa}) immediately. However, if we insist on fixing the texture on \overline{fab} along the \hat{z} direction, the only way to eliminate the accumulated vorticity is to create singularities at the surface. For example, we can collapse the entire loop $-\gamma_2-\gamma_1$ ($\gamma_1+\gamma_2$) along \overline{ab} (\overline{fa}) into the point a . (There may be other more favorable singularities. See discussions below.) This singular point now acts as a sink of the generated vorticity, and the textures in the rectangles $abcd$ and $fadef$ are nonaccumulating. Note that the boundary textures of $abcd$ (including the point

singularity at a) maps into the loop $(\gamma_1+\gamma_2-\gamma_2-\gamma_1)$ in S_i^2 , which covers no area. Hence we can always put into $abcd$ a texture $\hat{l}^0(x, z)$ that is deformable into the uniform texture $\hat{l}=\hat{z}$ (with the texture along the line segment \overline{abcd} held fixed along \hat{z} .⁸ From \hat{l}^0 , we can generate a nonaccumulating texture \hat{l}^1 in the entire cylinder Ω by defining $\hat{l}^1(r, z, \varphi)=\hat{l}^0(x=r, z)$, where r, z , and φ are cylindrical coordinates. It is clear that \hat{l}^1 and the uniform texture $\hat{l}=\hat{z}$ are topologically equivalent.

To prove the existence of nonaccumulating textures in closed containers with realistic boundary condition now becomes easy. Without loss of generality, the closed container can be taken as a sphere with the heat flow directed from the south pole S to the north pole N along the \hat{z} axis. Now we deform the textures in the bulk so that they become parallel to \hat{z} in a cigar-shaped volume that lies along the \hat{z} axis. This "uniform cigar" is then allowed to grow into a fat one (called F), pushing the original texture toward the surface, so that its tips are attached to N and S , and its volume occupies most of the bulk. (Create new surface singularities if necessary.) Since the cigars are just cylinders (topologically speaking), the uniform texture in F can be turned into a phase-slipping (hence time-dependent) and nonaccumulating one (i.e., with a surface singularity at N). The textures between the surfaces of F and the sphere remain time independent. This is possible because by construction, they match smoothly onto the uniform texture on the surface of F .¹¹

An example of a nonaccumulating texture $\hat{l}^0(x, z)$ in the cross section $abcd$ of the cylinder Ω in Fig. 1(a) at time $t=0$ is depicted in Fig. 2. The entire texture \hat{l}^1 in Ω is generated from \hat{l}^0 by defining $\hat{l}^1(r, z, \varphi)=\hat{l}^0(x=r, z)$. We assume that the discontinuities in the curvature on the surface give rise to the boundary texture as depicted.¹² The line segments \overline{dh} and \overline{ha} still map into γ_1 and γ_2 in S_i^2 as in Fig. 1(a). But instead of squeezing $-\gamma_2-\gamma_1$ down to point a , we collapse $-\gamma_2$ and $-\gamma_1$ separately into points s_1 and s_2 , which in turn generate two singular circles in \hat{l}^1 on the surface. The texture between the contours Λ_1 and Λ_2 precesses about \hat{z} in the negative sense, while that between Λ_2 and point a precesses in the positive sense. The texture between Λ_1 and the boundary $\overline{s_1bcd}$ is time independent, hence non-dissipative. They can be considered as being fixed by the strong anchoring of the surface. One will also recognize that as the sharp edges c and

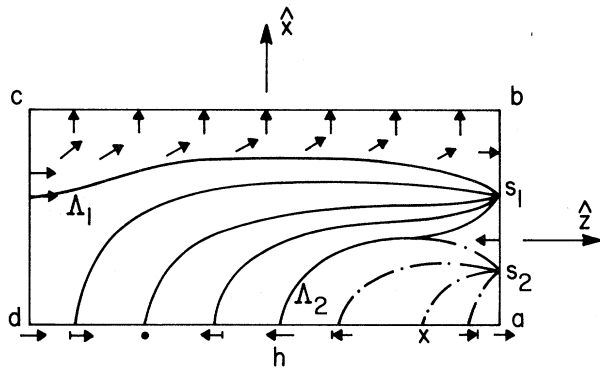


FIG. 2. A schematic representation of a nonaccumulating texture in the rectangle $abcd$ in Fig. 1(a) with the usual boundary condition. The solid and dotted lines represent contours of identical \hat{l} vectors. The \hat{l} vectors are represented in the same way as in Fig. 1(a).

b of the cylinder Ω are smoothed out, the singular circle generated by c corresponds to a boojum in a sphere at its infancy.³ It is quite plausible that the two circles s_1 and s_2 , instead of collapsing down to point a , will expand towards the edge b . Such an expansion will maximize the region of phase slippage as well as utilize the surface line singularity already present, instead of nucleating additional line or point singularities.¹³

Finally, I remark on some dynamic effects that are related to these topological considerations:

(a) I have deliberately put down one "soliton" in Fig. 2. The reason is that, for a reasonable heat flow $u = v_s - v_n \sim 10^{-3}$ cm/sec,¹ the length of one soliton in the bulk is roughly 0.1 cm. Containers with size ~ 0.5 cm can accommodate only a few solitons. To have a lot of solitons in the bulk, a large heat flow is required. Although my arguments on the existence of nonaccumulating textures remain valid, they also imply many singular lines on the surface. Whether this can be produced by magnetic field pulses or is dynamically less favorable than the boojum production remains unknown at the moment. In the limit when $v_n - v_s$ is very large, it is conceivable that both orbital and singular vortex phase slippage will contribute to dissipation.

(b) With the boundary texture shown in Fig. 2, the cylinder can just be filled with the uniform texture $\hat{l} = \hat{z}$ (to which the texture in Fig. 2 is topologically equivalent). Although there are no topological limitations, orbital phase slippage may be difficult to start with a uniform texture near T_c . This is because of the "accidental" stability of a uniform texture due to the nuclear di-

polar interaction.¹⁴ A nonuniform texture must be somehow produced (such as using a magnetic field as in Ref. 1). Our discussions imply that orbital precessions should be observed in both open and closed containers, once appropriate textures are established.

(c) I now consider the relation between heat flow and chemical-potential gradients. In our discussions, the surfaces $A = cde$ and $B = baf$ in Fig. 1(a) are considered as being kept at different temperatures T_A and T_B . As dictated by the relation $\mu = \partial f / \partial \rho$, where $f = f(T, \rho, \vec{v}_s, \hat{l}, \partial_i \hat{l}_j, \vec{g})$ is the free-energy density,⁶ and by the fact that A and B cannot be covered entirely by singularities, there must be a region of uniform \hat{l} in A and another in B with different μ , driving the texture into motion (or changing \vec{v}_s , and hence building up the kinetic energy) through (1). The time-dependent texture in Fig. 2 is another possible global solution of the hydrodynamic equations (besides boojum motion) which gives $[\partial_i v_s]_{av} = 0$ but does not suffer from surface pinning effects. At the surface, this solution is characterized by three connected regions mutually separated by two stationary singular loops s_1 and s_2 . Inside each connected surface region, μ is constant on the average, but undergoes discontinuous changes across the singular border. The latter is made possible because f , and hence μ , depends on $\nabla_i l_j$ and \hat{l} . The exact locations of the singular loops, like the actual forms of $\mu(r, t)$ and $T(r, t)$, depend on the solution of the hydrodynamic equations subject to the boundary condition of fixed surface temperatures T_A and T_B . Yet, no matter how complicated the solution is, as long as the boojum motion is not efficient enough the difference $T_A - T_B$ will induce textural "precessions" in the bulk, which in turn imply existence of surface singular loops if no distortions of \hat{l} are to be accumulated.

(d) At the surface, the chemical-potential gradient is balanced by the motions of \hat{l} concentrated at the singularities rather than by phase slippage, i.e., flow of vortex points (boojums). As a result, the time average of $\partial_i \vec{v}_s$ remains zero even if $\partial_i \hat{l}$ vanishes almost everywhere. The surface layer is not a conventional superfluid (as described by $\partial_i \vec{v}_s = \nabla \mu$, and $\vec{v}_s = \nabla \varphi$) across the singular border. It can be so described only within the connected regions bounded by singular loops.

I wish to thank those at NORDITA for their hospitality. This work was done at NORDITA and is supported by National Science Foundation Grant No. DMR 76-24011.

¹D. N. Paulson, M. Krusius, and J. C. Wheatley, Phys. Rev. Lett. **37**, 599 (1976).

²P. W. Anderson and G. Toulouse, Phys. Rev. Lett. **38**, 508 (1977).

³N. D. Mermin, Physica (Utrecht) **90B+C**, 1 (1977).

⁴H. E. Hall and J. R. Hook, J. Phys. C **10**, L91 (1977); J. R. Hook, to be published.

⁵V. Ambegoakar, P. G. de Gennes, and D. Rainer, Phys. Rev. A **9**, 2676 (1974).

⁶T. L. Ho, in *Quantum Fluids and Solids*, edited by S. Trickey *et al.* (Plenum, New York, 1977), p. 97.

⁷G. E. Volovik, Pis'ma Zh. Eksp. Teor. Fiz. **27**, 573 (1978) [JETP Lett. **27**, 605 (1978)].

⁸T. L. Ho, Phys. Rev. B **18**, 1144 (1978).

⁹Passage of a boojum on the surface or a 4π vortex (for definition, see Ref. 8) in the bulk across L means that an area 4π has been swept though by the line $\hat{l}(L)$ in S_1^2 .

¹⁰This configuration in the bulk, apart from some twisting along \hat{z} , corresponds to the $0-\pi-0$ soliton in Ref. 3. Note that when the rectangles $abcd$ and $adef$ in Fig. 1(a) cover the lower hemisphere of S_1^2 [Fig. 1(b)] once but with + and - orientation, they can be viewed as a pair of $\pm 2\pi$ vortices. The whole configuration in $adef$ is then deformable into an uniform one (see Ref. 8).

¹¹In our discussions, we have only talked about the textures but not the order parameters $\hat{\phi}$. The reason is that in simply connected containers, deformations of $\hat{\phi}$ subject to the usual boundary condition are characterized by the deformations of their textures. Suppose the textures \hat{l}_a and \hat{l}_b of order parameters $\hat{\phi}_a$ and $\hat{\phi}_b$ are connected by a deformation $\hat{l}_t = R(t)\hat{l}_a$, $0 \leq t \leq 1$, which satisfies the boundary condition for all t , where $R(t)$ is a rotational matrix satisfying $R(0) = 1$, $R(1)\hat{l}_a = \hat{l}_b$. Using the $\nabla \times \vec{v}_s$ equation [N. D. Mermin and T. L. Ho, Phys. Rev. Lett. **36**, 594 (1976)], it is easy to see that $\hat{\phi}_a' \equiv R(1)\hat{\phi}_a$ differs from $\hat{\phi}_b$ only by a phase factor $e^{i\chi}$. The family $\hat{\phi}^t = e^{it\chi} R(t)\hat{\phi}_a$ hence carries $\hat{\phi}_a$ continuously into $\hat{\phi}_b$.

¹²Our conclusions, however, do not depend on this particular choice of boundary texture.

¹³In case we change the boundary texture in Ω and put a boojum on the curved surface (the line \bar{bc} in Fig. 2), the texture between the contour Λ_1 and the boundary $s_1\bar{bcd}$ in Fig. 2 will then be time dependent because the boojum will move on the surface. However, the bulk texture (that enclosed by Λ_1) is still decoupled from that near the surface.

¹⁴P. Bhattacharyya, T. L. Ho, and N. D. Mermin, Phys. Rev. Lett. **39**, 1290, 1691(E) (1977).

Valley-Orbit Splitting of Li in Ge

A. Adolf, D. Fortier, and J. H. Albany

Laboratoire de Physique des Matériaux, Service de Chimie Physique, Centre d'Etudes Nucléaires de Saclay, 91190 Gif-sur-Yvette, France
and

K. Suzuki

Department of Electrical Engineering, Waseda University, Shinjuku, Tokyo

(Received 12 June 1978)

The thermal conductivity of germanium doped with lithium in the isolated impurity range has been measured between 0.4 and 20 K. The analysis of the electron-phonon scattering leads, for the first time, to a determination of the valley-orbit splitting (0.12 meV) of the ground state of the interstitial Li donor in Ge.

It is well known that in semiconductors phonon scattering by electrons bound to shallow impurities depends strongly on the electronic structure¹ of the latter. This was particularly emphasized in recent works on Li and other donors in silicon.²⁻⁵ Therefore phonon scattering is useful in the study of unknown impurity states. Among shallow donors in Ge and Si, only the ground state of a Li donor in Ge is still not known. The electronic structure of the ground state of Li in Si, which was suggested theoretically⁶ to be of the D_{3d} symmetry, was found^{7,8} to correspond to the T_d site with an "inverted" Group-V-like ground state and a valley-orbit splitting of 1.8

meV. The ground state of Li in Ge, which is fourfold degenerate in the effective-mass approximation, involves a singlet A_1 and a triplet T_2 in case of the T_d symmetry, and two singlets A_{2u} and a doublet E_u for the D_{3d} site. No convincing experimental evidence for a splitting of the ground state is so far available. However, the calculations of Nara and Yamazaki⁹ indicate that the ground state is expected, in the case of the T_d site, to exhibit an "inverted" structure (the triplet lying below the singlet) with a singlet-triplet interval of 0.15 meV, and to be nearly degenerate in the case of the D_{3d} symmetry. In this Letter, we present for the first time a determination of